




Thermal fluctuations assist mechanical signal propagation in coiled-coil proteinsJudit Clopés ¹, Jaehoh Shin ^{1,2}, Marcus Jahnel ^{3,4,5}, Stephan W. Grill,^{3,4,5} and Vasily Zaburdaev^{1,6,7,*}¹Max Planck Institute for the Physics of Complex Systems, Nöthnitzer Strasse 38, 01187 Dresden, Germany²Department of Chemistry, Rice University, Houston, Texas 77005, USA³Max Planck Institute of Molecular Cell Biology and Genetics, Pfotenhauerstrasse 108, 01307 Dresden, Germany⁴Biotechnology Center, Technical University Dresden, Tatzberg 47/49, 01307 Dresden, Germany⁵Cluster of Excellence Physics of Life, TU Dresden, Dresden, Germany⁶Friedrich-Alexander-Universität Erlangen-Nürnberg, Erlangen, Germany⁷Max-Planck-Zentrum für Physik und Medizin, Erlangen, Germany

(Received 30 April 2020; revised 15 October 2021; accepted 18 October 2021; published 11 November 2021)

Recently, it has been shown that the long coiled-coil membrane tether protein early endosome antigen 1 (EEA1) switches from a rigid to a flexible conformation upon binding of a signaling protein to its free end. This flexibility switch represents a motorlike activity, allowing EEA1 to generate a force that moves vesicles closer to the membrane they will fuse with. It was hypothesized that the binding-induced signal could propagate along the coiled coil and lead to conformational changes through the localized domains of the protein chain that deviate from a perfect coiled-coil structure. To elucidate, if upon binding of a single protein the corresponding mechanical signal could propagate through the whole 200-nm-long chain, we propose a simplified description of the coiled coil as a one-dimensional Frenkel-Kontorova chain. Using numerical simulations, we find that an initial perturbation of the chain can propagate along its whole length in the presence of thermal fluctuations. This may enable the change of the configuration of the entire molecule and thereby affect its stiffness. Our work sheds light on intramolecular communication and force generation in long coiled-coil proteins.

DOI: [10.1103/PhysRevE.104.054403](https://doi.org/10.1103/PhysRevE.104.054403)**I. INTRODUCTION**

Coiled-coils (CCs) are structural protein motifs composed of two or more intertwined α -helices. They play essential roles in multiple cellular processes, including gene regulation, muscle contraction, and cell signaling [1]. Early endosome antigen 1 (EEA1) is an extended fibrous protein with a large dimeric-CC domain that guides vesicles coated with the small GTPase Rab5 to early endosomes [2] [see Fig. 1(a)]. It has recently been shown that unbound EEA1 is rather stiff and becomes more flexible when active Rab5 selectively binds to its N-terminus [3] as measured by the almost fourfold decrease of the effective persistence length. The entropic force of the flexible chain brings the tethered vesicle closer to the endosome membrane to facilitate the downstream vesicle fusion. Next, guanosine triphosphate (GTP) hydrolysis breaks the interaction between EEA1 and Rab5, suggesting reversibility of this process. Similar behavior has been observed for other long CC tethering proteins, such as the golgin family [4–7], as well as in motor proteins. In dynein, for instance, the stalk

consists of a 15-nm-long dimeric CC that strongly changes its flexibility upon binding of adenosine triphosphate (ATP) [8]. Additionally, it has been shown that the dimeric CC in the *Streptococcus* M1 protein switches between two conformations due to destabilizing residues [9]. These observations show that CCs are not simply elastic rods playing a structural role inside cells, but are also functional allosteric molecules that can switch between diverse conformations and are controlled by ligands.

Structurally, the center part of EEA1 folds as a long canonical homodimeric CC of approximately 200 nm (1275 amino acids) on almost its total length [10] with a nearly straight conformation. The sequence of α -helices forming ideal left-handed CCs shows a periodic structural motif of *hpphppp* known as the heptad repeat, where *h* and *p* are the hydrophobic and polar residues, respectively [11]. In an aqueous environment, the CC fold is formed by the assembly of α -helices driven mainly by hydrophobic interactions established between the *h* residues of different strands. The regularity in the α -helix amino acid sequence of EEA1 is interrupted by short irregular regions distributed along the structure, which we will call discontinuities, where the amino acid sequences deviate from the heptad repeat periodicity. These irregularities yield short domains which have a lower probability of assembling as a coiled-coil structure [see Fig. 1(b)]. While the nature of the fold in these regions is not known, the recent findings have related the flexibility change with the presence of such discontinuities; the mutant EEA1 that lacks these regions does not show the stiffness switch [3].

*vasily.zaburdaev@fau.de

Published by the American Physical Society under the terms of the [Creative Commons Attribution 4.0 International](https://creativecommons.org/licenses/by/4.0/) license. Further distribution of this work must maintain attribution to the author(s) and the published article's title, journal citation, and DOI. Open access publication funded by the Max Planck Society.

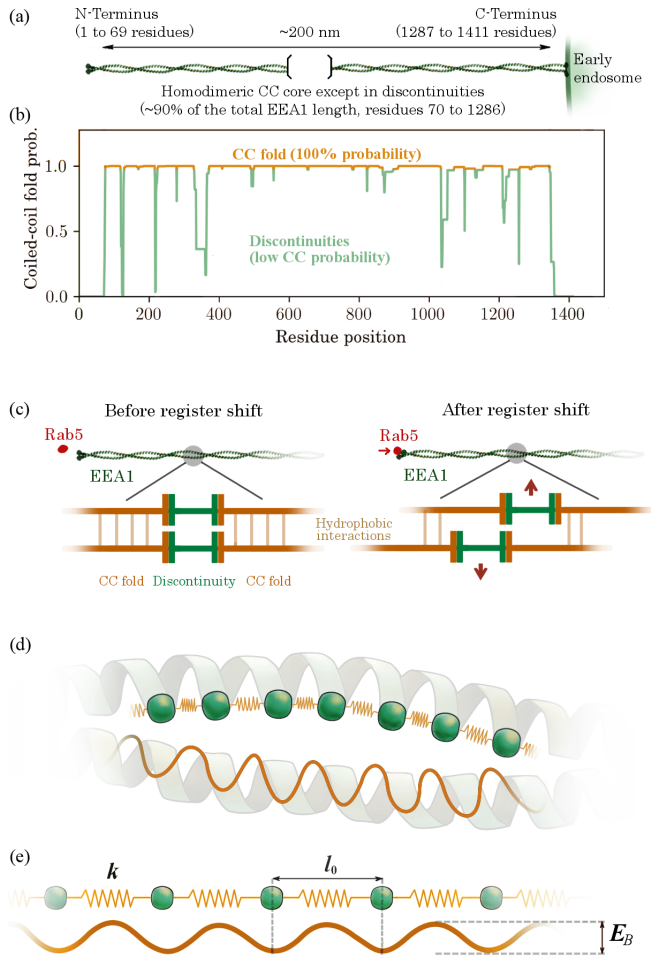


FIG. 1. Modeling hydrophobic interactions between strands in a canonical coiled-coil structure. (a) Sketch of the EEA1 structure. (b) Coiled-coil fold prediction for EEA1 in humans [16]. (c) Register shift between the α -helices of the EEA1 after Rab5 binding at the N-terminus. (d) Sketch of the application of the Frenkel-Kontorova model to map the hydrophobic contacts stabilizing the two α -helical strands forming a homodimeric canonical coiled-coil protein. (e) Frenkel-Kontorova model represented by a chain of beads connected by harmonic springs in the periodic potential. E_B and l_0 are the strength and the period of the hydrophobic interaction potential, respectively, where l_0 is also the half turn separating two hydrophobic residues and the equilibrium length of the harmonic spring (with the spring constant k) connecting two beads.

Therefore, we hypothesize that the ideal CC-fold regions could be involved in the energy transmission of the Rab5-EEA1 interaction through the whole structure whereas the discontinuities could be responsible for inducing the conformational change. We propose that binding of Rab5 introduces a mechanical perturbation in the form of a relative shift of two α -helices with respect to each other. When this shift happens within the CC-fold domain, it has no effect on the protein conformation. However, when the shift happens in the irregular domain, it effectively makes the region of the nonideal fold larger [see Fig. 1(c)]. We hypothesize that in an unperturbed state the discontinuity region still allows the protein to keep its stability in the highly persistent conformation [Fig. 1(c), left panel]. However, when the discontinuity

expands due to the shift and invades into the flanking ideal fold domains [Fig. 1(c), right panel] it could lead to the instability in the polymer conformation within these regions. To ensure energy transmission, the ideal CC regions in EEA1 must have a structure capable of propagating the perturbation with a sufficient signal amplitude to the discontinuity regions without destroying the dimeric-CC fold. At the same time, the perturbation should be able to travel through the discontinuity itself so that the shift could affect multiple discontinuities along the polymer contour to change its global conformation.

Different model approaches have addressed the unusual elastic properties of allosteric CCs. Flexibility differences in a dimeric-CC structure have been observed in a model composed by two flexible intertwined rods representing the α -helices' backbones. In this description, both bending and twisting vibrational modes are necessary to introduce changes in the global free energy of the CC upon ligand binding that are sufficiently large to be compatible with a flexibility allosteric transition [12]. However, in the EEA1 transition, the change in elasticity is not homogeneous but localized in rather short discontinuities of the CC pattern [3]. A reminiscent behavior to that in the EEA1 has been suggested for single α -helices when affected by stresses along or perpendicular to the long axis of the peptide. Above a certain force threshold, helical polymers such as α -helices bend at specific points along its length, which soften the structure overall, although the flexibility distribution along the molecule is rather heterogeneous [13,14]. Relatedly, the structural response of CC to applied forces, including the amplification of small perturbations, has been also observed in molecular dynamics simulations in a mechanoelastic canonical CC model [15]. These studies suggest possible underlying mechanisms of the flexibility switch in CC structures upon application of force, e.g., due to a ligand binding, assuming that the perturbation at one end has propagated through the whole CC and a new equilibrium state is immediately established. In contrast to the above work, the main question addressed here is the study of the intramolecular propagation dynamics of a perturbation starting at one end of the CC through the protein's whole structure within the biologically relevant time [3].

To investigate the feasibility of such an energy transmission mechanism from the physical point of view, we applied an overdamped one-dimensional Frenkel-Kontorova (FK) model [18] to a range of problems of signal transduction. We analyzed the dynamics of dislocations in FK chains for the length scales and timescales characteristic of the EEA1 protein, and we find that thermal fluctuations are necessary for the signal to propagate through the whole structure. Moreover, we provide the range of parameters when such signal propagation is feasible within the experimentally measured time. Finally, based on our results, we briefly discuss how a small perturbation can trigger the change of the global properties of EEA1.

II. THE FRENKEL-KONTOROVA MODEL APPLIED TO COILED-COIL STRUCTURES

The hydrophobic interactions between strands in an ideal CC fold can be described in terms of a one-dimensional FK chain [18] [see Figs. 1(d) and 1(e)]. The original FK model

was introduced in the late 1930's to describe defect dynamics in solids. In the context of biological systems, it has been used to model phenomena such as friction [19,20], protein folding [21], chromatin dynamics [22], and DNA breathing [23].

When applied to CCs, this model is coarse grained to the hydrophobic residue level, where each heptad repeat is described by two beads connected by a spring. The periodic potential with amplitude E_B and period l_0 characterizes the strength of the hydrophobic interaction between residues of opposite strands. Since the two α -helices forming the dimeric CC in EEA1 have an identical amino acid sequence and align in parallel [10], the effect of the hydrophobic interactions in the FK chain was chosen to be commensurate where the equilibrium length of the springs l_0 coincides with the potential period. We note that for the wild-type EEA1 CC with discontinuities, the hydrophobic interactions will not be perfectly periodic. The elastic constant k of the spring connecting two neighboring beads is related to the contributions from both the rigidity at small stretches and the hydrogen bonds established between the third and fourth nearest neighbors in α -helices (half heptad repeat).

We introduce the Rab5-EEA1 interaction as a register shift, i.e., a relative sliding of half a heptad repeat in one α -helix with respect to the other. This mechanism could introduce long-distance communication along the CC fold at a low energetic cost, since it does not involve the exposure of hydrophobic residues to the aqueous environment [see Fig. 1(c)]. Register shifts have been suggested as a mechanism responsible for the allosteric communication along the homodimeric CC forming the stalk of dynein [24,25], and is also involved in signal transmission along transmembrane proteins [26]. Below, we first show that thermal fluctuations are necessary to ensure the propagation of an initial perturbation on one extreme through the whole length of the chain. Then, we study the chain parameters which allow for the signal transmission and relate these results to the EEA1 protein. We conclude by discussing how the presence of a discontinuity might affect the signal propagation.

We have modeled the canonical coiled-coil regions in EEA1 by means of an overdamped FK chain. The equation of motion for the i th bead in terms of Langevin dynamics is

$$\gamma \frac{dx_i(t)}{dt} = -\frac{\partial U_i(t)}{\partial x_i} + \xi_i(t), \quad (1)$$

where $x_i(t)$ is the position of the bead, γ is the friction introduced by both the medium and the interaction between opposite strands, and $\xi_i(t)$ is a Gaussian white noise describing thermal fluctuations, satisfying $\langle \xi_i(t) \rangle = 0$ and $\langle \xi_i(t) \xi_j(t') \rangle = 2\gamma k_B T \delta(t - t') \delta_{i,j}$. The potential energy $U_i(t)$ is given by

$$U_i(t) = \frac{-E_B}{2} \cos\left(\frac{2\pi x_i}{l_0}\right) + \frac{k}{2} [(x_{i+1} - x_i - l_0)^2 + (x_{i-1} - x_i - l_0)^2]. \quad (2)$$

The initial perturbation from Rab5 binding is introduced by generating a compression (kink) of length l_0 between the leftmost pair of beads of the FK chain and keeping the position of the first bead fixed. This leads to an excess of

the elastic energy due to the register shift. We then analyzed the dynamics of the potential energy distribution per bead on the FK chain $U_i(t)$. The signal propagation analysis was performed by averaging single kink trajectories for kinks introduced in one of the extremes and in the center of the chain. The signals were postprocessed using the Savitzky-Golay filter [27]. We then analyzed the propagation front x_{fr} [see Fig. 2(c)], defined as the length at which the filtered signal amplitude reaches the threshold energy, which is the mean energy of the beads introduced solely by temperature in a resting chain.

III. CHARACTERIZATION OF THE SIGNAL TRANSMISSION

The energy transport along the FK chain is a result of two processes: the relaxation of the contraction and a diffusive propagation of the kink due to thermal effects.

In the absence of thermal fluctuations, or at low temperature, the contraction applied to the extreme affects only a limited region of the chain with a characteristic size $\lambda = l_0^2 \sqrt{k/E_B}$ [18,19], known as the kink width, and does not propagate further [see Fig. 2(a)]. The chain rapidly reaches a new equilibrium configuration, where the elastic energy accumulated by the register shift $\delta U = kl_0^2/2$ is either dissipated or redistributed along the few monomers of the chain.

Importantly, at intermediate temperatures ($U_i \gtrsim k_B T$), thermal fluctuations assist the chain monomers in crossing the potential barrier enabling further propagation of the energy. A single kink diffuses while maintaining a constant kink width. The relaxation of the kink due to the elastic and viscous forces occurs much faster than the characteristic time of the stochastic kink hopping over the potential barriers. As a result, these two phenomena can be decoupled [28] leading to diffusion-dominated transport of energy at large timescales. Too high temperatures ($U_i < k_B T$) would melt the coiled-coil structure by spontaneously generating kink-antikink pairs along the chain and thus also abrogate the transport.

The kink jumps are more frequent as the bond energy E_B (potential barrier) decreases, so the overall diffusive signal propagation is faster for decreasing E_B . Furthermore, the propagation is enhanced in stiffer chains, i.e., by increasing the elastic constant k , since the energy introduced in the initial perturbation is greater [see Fig. 2(c)]. This phenomenon is reminiscent of the motion of a Brownian particle or a polymer in a tilted washboard potential [29]. The register shift in our model plays a similar role of tilting the potential.

The potential energy distribution at chain positions away from the boundary $x > \lambda$ shows a diffusive evolution at large times [see Fig. 2(b)]. We consider the time evolution of the energy peak at x_{pk} at $t = 0$ with the reflecting boundary at $x = 0$. We obtain the corresponding solution of the diffusive equation using the method of image,

$$P(x \geq 0, t) = \frac{A_0}{\sqrt{4\pi Dt}} \left\{ \exp\left[\frac{-(x - x_{pk})^2}{4Dt}\right] + \exp\left[\frac{-(x + x_{pk})^2}{4Dt}\right] \right\}, \quad (3)$$

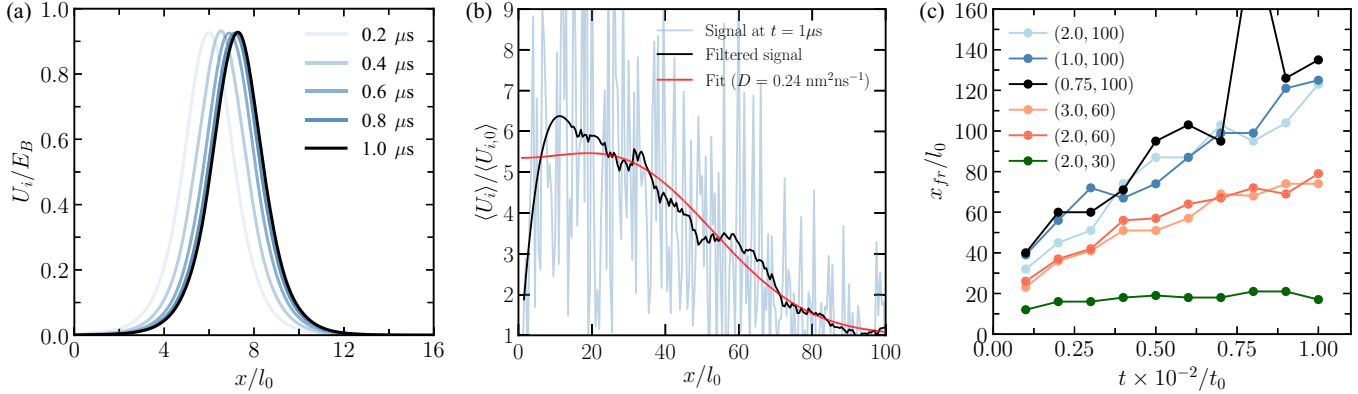


FIG. 2. Signal propagation analysis. (a) Evolution of the potential energy distribution profile along a Frenkel-Kontorova chain in the absence of thermal fluctuations with $E_B = 1k_B T$ and $k = 100k_B T \text{ nm}^{-2}$. The initial contraction relaxes and does not propagate. (b) Potential energy distribution profile averaged over 5000 trajectories for identical chains affected by thermal fluctuations, normalized by the average energy per bead in a chain without perturbations, $\langle U_i \rangle$. In this case, the compression is active and propagates diffusively. The averaged signal has been filtered by applying the Savitzky-Golay algorithm with a window size of 51 data points [27] (black). The fit curve (red) corresponds to the solution to the diffusion equation with a reflecting boundary at $x = 0$ with the diffusion constant D extracted from the fit. (c) Dynamics of the position of the potential energy front x_{fr} for different E_B and k pairs, indicated in brackets. The front position x_{fr} is the position where the filtered signal reaches the threshold. The units of E_B and k are $k_B T$ and $k_B T \text{ nm}^{-2}$, in all plots, respectively, where T is the room temperature.

where A_0 is the normalization constant. By using this formula [red line in Fig. 2(b)], we extract the diffusion constant D of the kink. In our situation, x_{pk} is expected to be very close to the reflecting boundary, at the distance of the order of the kink width. For simplicity, we do not specify this value and just use it as an additional fitting parameter.

IV. RELATION TO THE CASE OF THE EEA1 COILED-COIL PROTEIN

The parameter set used to reproduce the physiological conditions at which CC proteins are functional is listed in Table I. The equilibrium distance between two beads corresponds to the length of a turn in canonical CCs, l_0 , which has an approximate value of 0.5 nm [30,31]. The range of the elastic constant k corresponds to the stretching of coiled-coil regions of myosin in the limit of small pulling forces, where the elasticity is entropic, until the first hydrogen bond in the α -helix (half heptad repeat) is broken at roughly $k_0 = 65k_B T \text{ nm}^{-2}$ [32], where $T = 300 \text{ K}$ is the room temperature, which is consistent with the maximum longitudinal bending stiffness of the tropomyosin coiled-coil used in Ref. [15].

TABLE I. Choice of biologically relevant parameters for the Frenkel-Kontorova model applied to describe ideal coiled-coil structures.

Parameter	Range	Reference
Turn length L, l_0	0.5 nm	[30,31]
Chain length N	400 beads	[38]
Hydrophobic int. E_B	$< 4k_B T$	[35]
Elastic constant k	$1-65k_B T \text{ nm}^{-2}$	[15,32,33]
Dyn. water viscosity η_w	$0.85 \text{ pN ns nm}^{-2}$	[34]
Activation energy E_A	$< 20k_B T$	[39]

For short peptide chains, the elastic constant k is reduced to values around $40k_B T \text{ nm}^{-2}$ [33]. The friction coefficient γ is estimated using the Stokes law $\gamma = 6\pi\eta R$ with the dynamic viscosity of water at 300 K, $\eta_w = 0.85 \text{ pN ns nm}^{-2}$ [34], and assuming the amino acid radius R to be of the order of $l_0/2$. We estimate a maximum strength of the hydrophobic interactions of $4k_B T$, that corresponds to the hydration potential of isoleucine [35], although accurate measurements of the solvation free energies of biomolecules are difficult to access experimentally [36,37]. Since the CC structure is not melting, but sliding, this value for E_B might be overestimating the hydrophobic interaction established between the residues of opposite strands. Similarly, the energy required for transferring buried residues from the interior to the protein surface is much lower than its full solvation [35]. Since the Rab5-EEA1 interaction and the consequent signal propagation occur without GTP hydrolysis [3], an upper limit for the activation energy E_A is $20k_B T$.

The ranges of k and E_B that would allow the signal to propagate until the opposite end of the EEA1 protein are shown in Fig. 3. The diffusion constant D has been obtained by fitting the solution to diffusion equation (Gaussian distribution) in an unbounded domain to the average of 2000 kink trajectories generated at the center of the chain. The diffusion constant D for kinks introduced both at the center and at the extreme of the chain are equivalent in the long-time limit. We note that for the case of a single particle in a periodic potential, we may estimate the diffusion constant by using the Kramers' argument. Indeed, it gives a qualitatively similar trend to the simulation data of the FK chain (data not shown). However, the quantitative behavior is radically different because neighboring monomers in the FK chain tend to move simultaneously due to mechanical coupling.

The sum of the energy contributions required to overcome the potential barrier E_B , and to compress the first monomer

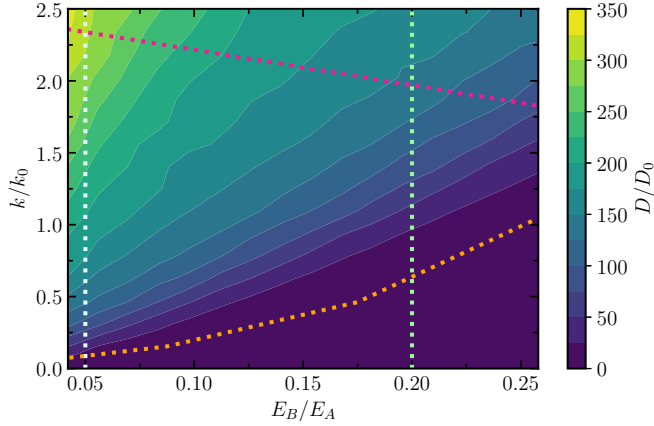


FIG. 3. Diffusion coefficient of a kink generated in the center of a Frenkel-Kontorova chain for different chain stiffness k and bond energy E_B , each extracted from the energy average of 2000 kink trajectories, normalized by the minimum diffusion constant required to transmit the signal, D_0 , the maximum chain stiffness, $k_0 = 65k_B T \text{ nm}^{-2}$, and the maximum activation energy, $E_A = 20k_B T$. The upper limit (magenta) corresponds to the limit where the activation energy cannot overcome the first potential barrier. The orange line limits the cases where the diffusion constant is D_0 . Hydrophobic bond energy differences E_B below $1k_B T$ ($E_B/E_A = 0.05$) lead to unstable chains (white). Finally, the maximum energy released between a pair of hydrophobic residues E_B is approximately $4k_B T$ ($E_B/E_A = 0.2$) [35] (light green).

to a length l_0 , must not surpass the energy released by the hydrolysis of a GTP molecule ($\approx 20k_B T$),

$$\frac{1}{2}kl_0^2 + E_B \leq 20k_B T. \quad (4)$$

This provides an upper limit for the values of the elastic constant k and the bond energy E_B (shown in orange). The time required to complete a full EEA1-Rab5 cycle is around $t_c = 0.1 \text{ s}$ [3]. This delimits the minimum required signal speed according to $t_c \geq \langle N^2 \rangle / 2D$, where N is the length of the chain. From the results shown in Fig. 3 and the physiological parameters in Table I, we predict the ranges for the hydrophobic interaction energy $E_B \in (1.0, 4.0)k_B T$ and an elasticity range of $k \in [10, 150]k_B T \text{ nm}^{-2}$ to $k \in [10, 125]k_B T \text{ nm}^{-2}$ depending on E_B , allowing for signal propagation in EEA1 at physiological conditions. Hydrophobic contacts E_B with less than $1k_B T$ lead to unstable chains due to the spontaneous generation of kink-antikink pairs already observed in the results (white dotted line).

V. CONCLUSIONS

How a local interaction affects the global property of a molecule is an important question in physical and biological systems. Recent experiments on the membrane tether EEA1 have shown that binding of the small GTPase Rab5 to the N-terminus of EEA1 significantly reduces the bending stiffness of this long coiled-coil protein. To elucidate this phenomenon, we proposed a simplified description of the CC as a finite-length FK chain, modeling ligand binding as a register shift. Using numerical simulations, we found that the signal can reach the other end of the chain only in the presence

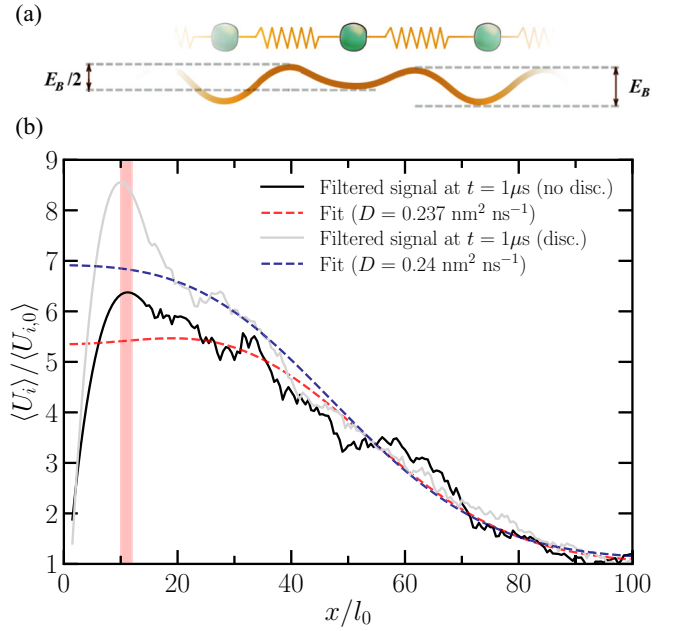


FIG. 4. (a) Sketch of the discontinuity model. (b) Potential energy distribution profile at $t = 1 \mu\text{s}$ averaged over 5000 trajectories for chains with $E_B = 1k_B T$ and $k = 100k_B T \text{ nm}^{-2}$ affected by thermal fluctuations, which include a discontinuity (light gray line) affecting the region highlighted in light red, normalized by the average energy per bead in a chain without perturbations, $\langle U_{i,0} \rangle$. This distribution is compared with that of a chain with the same k , E_B properties which does not have a discontinuity (black line), discussed in Fig. 2(b). Both filtered signals have been obtained by applying the Savitzky-Golay algorithm with a window size of 51 data points [27] on the original signal averages. The fits (dashed lines, red and blue for the no-discontinuity and discontinuity cases, respectively) correspond to the solution to the diffusion equation with a reflecting boundary at $x = 0$ with the indicated diffusion constant D values extracted from the fit.

of thermal fluctuations. Importantly, we determine the range of parameters that enable the intramolecular communication within the experimentally estimated time; those can be used to predict the elastic parameters and the hydrophobic interaction strength of the EEA1 CC.

It is worth noting that due to the simplicity of the model, we neglect a few features of the original system. First, while the CCs are three-dimensional (3D) objects, we have treated them as being effectively one dimensional. Since the ratio of length and diameter of EEA1 is ~ 100 , all the vibrational motions along the radial (transverse) direction are much faster than along the protein contour. We can thus assume that all the radial motions are averaged out as the signal propagation is a much slower process. With this simplification, however, the bending stiffness of the CC is not explicitly taken into account. Therefore, the question of how bending stiffness changes remains an open problem. Instead, the main focus of our study is on how the signal propagates along the long CC chain.

Second, while we considered a signal propagation through an ideal CC, a natural question arises whether the discontinuities themselves could hinder the signal propagation. Thus we also tested whether signal propagation is still possible in

the presence of a “discontinuity.” Since the precise molecular nature of the discontinuity is not known, we model it in a relatively simplistic manner: by a single potential period of half depth of the normal case. The physical reason is that while the hydrophobic interaction weakens at a discontinuity, the electrostatic interaction still exists. Similarly, this size of the discontinuity domain in the FK model roughly corresponds to the size of a discontinuity from CC-fold data [see Fig. 1(b)]. In this setting, we find that signal propagation is only modestly hindered (see Fig. 4). We therefore suggest that while the discontinuity does not affect the signal propagation along the chain, it can promote the conformation change. As illustrated in Fig. 1(c), the register shift increases the size of the nonideal fold. This can lead to the conformation change at many discontinuities along the protein contour decreasing its local bending stiffness and globally decrease protein persistence length. Our results also indicate that the EEA1 is in the vicinity of the critical point between stable (stiff) and unstable (flexible) states where the ligand binding can trigger flexibility transition but only in the presence of thermal fluctuations. This phenomenon is another illustration of the common dual role of thermal fluctuations in biological systems [40]: While too large thermal fluctuations can make the system unstable,

too small thermal fluctuations cannot lead to the flexibility transition. In other words, thermal fluctuations are not “harmful” to the CC, but, in this case, essential for its biological function.

Lastly, we note that while the conformation changes of relatively short CCs (≈ 10 nm) have been investigated in many experimental studies, there are only a few studies for longer CCs. To further investigate the signal transduction mechanism in the EEA1, we propose to chemically cross-link the two α -helices at different sites [41], for example, at the seven distinct cysteine residues located within the predicted coiled-coil region. The cross-linking would prevent signal propagation, and hence the flexibility transition would not occur. In this way, one could test the idea of thermal noise-induced signal propagation along EEA1 CC and thus would be an important step for experimental verification of the theoretical predictions of this work.

ACKNOWLEDGMENTS

We acknowledge helpful discussions with M. Zerial and D. Murray. This research was supported by the Max Planck Society.

-
- [1] A. N. Lupas and J. Bassler, Coiled coils—a model system for the 21st century, *Trends Biochem. Sci.* **42**, 130 (2017).
- [2] F.-T. Mu, J. M. Callaghan, O. Steele-Mortimer, H. Stenmark, R. G. Parton, P. L. Campbell, J. McCluskey, J.-P. Yeo, E. P. C. Tock, and B.-H. Toh, EEA1, an early endosome-associated protein, *J. Biol. Chem.* **270**, 13503 (1995).
- [3] D. H. Murray, M. Jahnel, J. Lauer, M. J. Avellaneda, N. Brouilly, A. Cezanne, H. Morales-Navarrete, E. D. Perini, C. Ferguson, A. N. Lupas, Y. Kalaizidis, R. G. Parton, S. W. Grill, and M. Zerial, An endosomal tether undergoes an entropic collapse to bring vesicles together, *Nature (London)* **537**, 107 (2016).
- [4] T. M. Witkos and M. Lowe, The golgin family of coiled-coil tethering proteins, *Front. Cell. Dev. Biol.* **3**, 1 (2016).
- [5] C. A. Laughton, B. F. Luisi, J. V. Pratap, and C. R. Calladine, A potential molecular switch in an alpha-helical coiled-coil, *Proteins* **70**, 25 (2007).
- [6] A. K. Gillingham and S. Munro, Long coiled-coil proteins and membrane traffic, *BBA-Mol. Cell Res.* **1641**, 71 (2003).
- [7] A. K. Gillingham, At the ends of their tethers! How coiled-coil proteins capture vesicles at the golgi, *Biochem. Soc. Trans.* **46**, 43 (2018).
- [8] S. A. Burgess, M. L. Walker, K. Thirumurugan, J. Trinick, and P. J. Knight, Use of negative stain and single-particle image processing to explore dynamic properties of flexible macromolecules, *J. Struct. Biol.* **147**, 247 (2004).
- [9] C. M. Stewart, C. Z. Buffalo, J. A. Valderrama, A. Henningham, J. N. Cole, V. Nizet, and P. Ghosh, Coiled-coil destabilizing residues in the group A *Streptococcus* M1 protein are required for functional interaction, *Proc. Natl. Acad. Sci. USA* **113**, 9515 (2016).
- [10] J. Callaghan, A. Simonsen, J.-M. Gaullier, B.-H. Toh, and H. Stenmark, The endosome fusion regulator early-endosomal autoantigen 1 (EEA1) is a dimer, *Biochem. J.* **338**, 539 (1999).
- [11] C. Cohen and D. A. D. Parry, α -helical coiled coils a widespread motif in proteins, *Trends Biochem. Sci.* **11**, 245 (1986).
- [12] R. J. Hawkins and T. C. B. McLeish, Dynamic allostery of protein alpha-helical coiled-coils, *J. R. Soc., Interface* **3**, 125 (2006).
- [13] P. Palenčár and T. Bleha, Molecular dynamics simulations of the folding of poly (alanine) peptides, *J. Mol. Model.* **17**, 2367 (2011).
- [14] P. Palenčár and T. Bleha, Bending and kinking in helical polymers, *J. Polym. Sci., Part B: Polym. Phys.* **53**, 1345 (2015).
- [15] O. N. Yagci, C. Wolgemuth, and S. X. Sun, Mechanical response and conformational amplification in alpha-helical coiled coils, *Biophys. J.* **99**, 3895 (2010).
- [16] Coiled-coil fold prediction computed with the PCOILS bioinformatics toolkit for left-handed coiled coils [17] using an averaging window of 28 amino acids. The window size corresponds to the value recommended by the tool authors, which includes a sequence of four heptad repeats.
- [17] L. Zimmermann, A. Stephens, S.-Z. Nam, D. Rau, J. Kbler, M. Lozajic, F. Gabler, J. Sding, A. N. Lupas, and V. Alva, A completely reimplemented MPI bioinformatics toolkit with a new HHpred server at its core, *J. Mol. Biol.* **430**, 2237 (2018).
- [18] O. M. Braun and Y. S. Kivshar, *The Frenkel-Kontorova Model* (Springer, Berlin, 1987).
- [19] A. Ward, F. Hilitski, W. Schwenger, D. Welch, A. W. C. Lau, V. Vitelli, L. Mahadevan, and Z. Dogic, Solid friction between soft filaments, *Nat. Mater.* **14**, 583 (2015).
- [20] A. Vanossi, N. Manini, and E. Tosatti, Static and dynamic friction in sliding colloidal monolayers, *Proc. Natl. Acad. Sci. USA* **109**, 16429 (2012).
- [21] A. K. Sieradzka, A. Niemi, and X. Peng, Peierls-Nabarro barrier and protein loop propagation, *Phys. Rev. E* **90**, 062717 (2014).

- [22] I. M. Kulić and H. Schiessel, Chromatin Dynamics: Nucleosomes Go Mobile through Twist Defects, *Phys. Rev. Lett.* **91**, 148103 (2003).
- [23] A. Sulaiman, F. P. Zen, H. Alatas, and L. T. Handoko, Dynamics of DNA breathing in the Peyrard-Bishop model with damping and external force, *Physica D* **241**, 1640 (2012).
- [24] K. Hirose and L. A. Amos, *Handbook of Dynein* (CRC, Boca Raton, FL, 2012).
- [25] T. Kon, K. Imamula, A. J. Roberts, R. Ohkura, P. J. Knight, I. R. Gibbons, S. A. Burgess, and K. Sutoh, Helix sliding in the stalk coiled coil of dynein couples atpase and microtubule binding, *Nat. Struct. Mol. Biol.* **16**, 325 (2009).
- [26] E. E. Matthews, M. Zoonens, and D. M. Engelman, Dynamic helix interactions in transmembrane signaling, *Cell* **127**, 447 (2006).
- [27] A. Savitzky and M. J. E. Golay, Smoothing and differentiation of data by simplified least squares procedures, *Anal. Chem.* **36**, 1627 (1964).
- [28] N. R. Quintero, Á. Sánchez, and F. G. Mertens, Overdamped sine-Gordon kink in a thermal bath, *Phys. Rev. E* **60**, 222 (1999).
- [29] G. Costantini and F. Marchesoni, Threshold diffusion in a tilted washboard potential, *Europhys. Lett.* **48**, 491 (1999).
- [30] F. H. C. Crick, Is alpha-keratin a coiled-coil? *Nature (London)* **170**, 882 (1952).
- [31] L. Truebestein and T. A. Leonard, Coiled-coils: the long and short of it, *Bioessays* **38**, 903 (2016).
- [32] D. D. Root, V. K. Yadavalli, J. G. Forbes, and K. Wang, Coiled-coil nanomechanics and uncoiling and unfolding of the superhelix and alpha-helices of myosin, *Biophys. J.* **90**, 2852 (2006).
- [33] M. A. Lantz, S. P. Jarvis, H. Tokumoto, T. Martinsky, T. Kusumi, C. Nakamura, and J. Miyake, Stretching the α -helix: A direct measure of the hydrogen-bond energy of a single-peptide molecule, *Chem. Phys. Lett.* **315**, 61 (1999).
- [34] IAPWS, *IAPWS Industrial Formulation 2008 for the Thermodynamic Properties of Water and Steam*, International Steam Tables (Springer, Berlin, 2008).
- [35] R. Wolfenden, L. Andersson, P. M. Cullis, and C. C. B. Southgate, Affinities of amino acid side chains for solvent water, *Biochemistry* **20**, 849 (1981).
- [36] G. König, S. Bruckner, and S. Boresch, Absolute hydration free energies of blocked amino acids: Implications for protein solvation and stability, *Biophys. J.* **104**, 453 (2013).
- [37] A. Nicholls, D. L. Mobley, J. P. Guthrie, J. D. Chodera, C. I. Bayly, M. D. Cooper, and V. S. Pande, Predicting small-molecule solvation free energies: An informal blind test for computational chemistry, *J. Med. Chem.* **51**, 769 (2008).
- [38] The UniProt Consortium, UniProt: the universal protein knowledgebase in 2021, *Nucleic Acids Res.* **49**, D480 (2021).
- [39] D. L. Nelson and M. M. Cox, *Lehninger Principles of Biochemistry*, 7th ed. (W. H. Freeman, New York, 2017).
- [40] M. A. Munoz, Colloquium: Criticality and dynamical scaling in living systems, *Rev. Mod. Phys.* **90**, 031001 (2018).
- [41] A. Snoberger, E. J. Brettrager, and D. M. Smith, Conformational switching in the coiled-coil domains of a proteasomal ATPase regulates substrate processing, *Nat. Commun.* **9**, 2374 (2018).